WALAILAK JOURNAL
http://wjst.wu.ac.th Engineering and Physical Sciences

A Numerical Study of Load Distribution of Pile Group Foundation by 2D Model

Boonchai UKRITCHON*, Janine FAUSTINO and Suraparb KEAWSAWASVONG

Department of Civil Engineering, Chulalongkorn University, Bangkok 10330, Thailand

(*Corresponding author's e-mail: boonchai.uk@gmail.com)

Received: 11 June 2015, Revised: 26 October 2015, Accepted: 11 November 2015

Abstract

Studies about pile group foundation have been rapidly increasing in number over the past years. However, past research works focused on pile settlement with consideration of a purely vertical load for pile groups or pile raft foundations. There were few studies with an emphasis on pile load distribution of pile group foundations together with a combined vertical load and a large overturning moment. For example, the foundation of a wind turbine carries a large overturning moment and vertical forces at the base of the structure. This paper presents a numerical study of load distribution of pile group foundations. A 2D numerical model using finite element software, PLAXIS 2D, has been employed to analyze the behavior of the pile group foundation. In the scope of analysis, pile group foundation consisting of large numbers of regular grid piles with a cross section of the strip of the pile row can be analyzed with a 2D model. For structural modeling, each pile is modeled as the embedded pile row. Modeling of pile group foundation is achieved by creation of a small gap between the plate element of the pile cap and the underlying soil, while the pile cap is rigidly connected with a small vertical plate segment which is hinged at the top of the embedded pile row. Several parametric studies, including numbers of piles, overturning moment ratios, stiffness of pile cap, and pile spacing, are also presented in this paper.

Keywords: Numerical analysis, pile group, finite element, load distribution

Introduction

In foundation design, shallow foundations are customarily considered first, to support structural loads. If shallow foundations are not adequate, deep foundations are used instead, to utilize the bearing capacity of stronger soil layers, which are normally located at deeper stratum. In most practical situations, such as constructing large structures, piles are used in groups (pile group foundation). The layout can come in any type of geometrical pattern (square, circle, rectangle, etc.) with spacing, S (center-to-center distance between piles). Structural loads are transferred to the pile group by means of a pile cap, which is connected to the head of each pile. When the pile group foundations are designed so that loadings are transmitted to only piles, not underlying soil through contacted raft, the pile load distribution can be calculated according to most foundation handbooks (e.g. Bowles [1]) as;

$$F_i = \frac{P}{N} \pm \frac{M_y x_i}{\sum {x_i}^2} + \frac{M_x y_i}{\sum {y_i}^2} \quad (1)$$

where P = vertical applied load
N = numbers of piles
M_x, M_y = moments about x axis and y axis, respectively
x_i, y_i = distances of the pile i from x axis and y axis and
Σx_i^2, Σy_i^2 = moment of inertia of the pile group about x axis and y axis, respectively

Eq. (1) stems from the major assumptions: 1) the pile group foundation is modeled as a fully rigid pile cap; 2) all piles are modeled as springs of the same stiffness; and 3) the base of the springs must be fully rigid without any settlement, as shown in **Figure 1**. On the other hand, another type of analysis, the flexible pile cap, may be adopted, by assuming that the pile cap may not behave rigidly, but depends on its flexural stiffness, EI. Structural analysis, which considers both the cap stiffness and spring stiffness, must be performed for this case. As a result, the pile load distribution of the flexible cap case may be different from that of the rigid cap case.

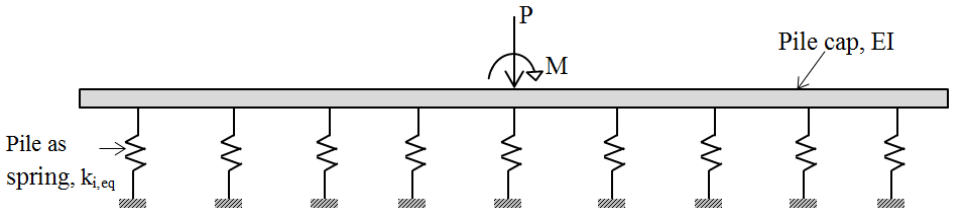

Figure 1 Classical analysis of pile group foundation.

In reality, the settlement of a pile group is equal to the sum of the elastic shortening of the pile, displacement due to shearing around the pile shaft, and displacement of the end bearing point, together with some interaction effects between adjacent piles. The latter is called the pile group effect. Thus, pile load distribution, individual pile settlement, and soil displacement must be analyzed, using such methods as that of finite element, where 3D geometry of the problem, including the cap and geometrical position of the pile, must be considered in the analysis.

However, there are some situations where analyses of the pile group can be approximated using a 2D finite element model, as shown in **Figure 2**. In this situation, the pile group foundation consists of so many regular grid piles that the vertical cross section, considering the strip of pile row, can be analyzed by a 2D model. In addition, loading conditions of the pile group may be a purely vertical load and/or combined vertical load, with a uniaxial bending moment. More importantly, series of pile rows must be modeled with a special element which allows soil to move around it, and not be constrained by plane strain condition in the 2D model. Without this special element, the 2D modeled piles behave as continuous walls and, thus, the approximation is not valid. Recently, PLAXIS 2D, (Brinkgreve [2]), the finite element software, has developed this special element, called the embedded pile row, where 3D pile group foundations can be approximated by 2D models, shown in **Figure 2**. Various researchers have studied pile group foundations. However, most of them focused on the settlement of pile groups with purely vertical loads. The case of pile load distribution in pile group foundations and combined vertical loads and moments have been studied by very few. Thus, the aim of this paper is to study the pile group foundation by approximation of the 2D finite element, together with an embedded pile row in PLAXIS 2D, in order to understand pile load distribution when subjected to combined vertical loads and large overturning moments.

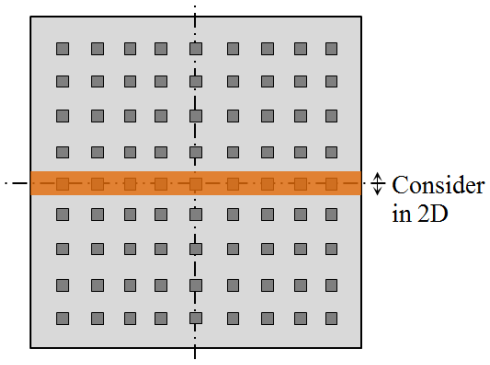

Figure 2 Pile group foundation studied by 2D model.

Some researchers have already used embedded pile rows to study pile group foundation. For example, Engin *et al.* [6] studied the behavior of a single pile and pile group foundation using an embedded pile row. It showed that it had similar behavior with the field test data, in both the compression test and the pullout test. The influence of pile spacing was also observed in the behavior of the pile group, in terms of a load-displacement curve. It was found that, as the spacing between piles increased, the load that the pile group could carry to produce the same settlement also increased. This kind of numerical analysis was also performed by Comodromos *et al.* [4]. Their results showed that, by decreasing the spacing of the piles, the interaction between them increased; therefore the stiffness of each pile decreased. In a study made by Lebeau [7], an embedded pile was used to analyze the influence of skin friction distribution in the behavior of the pile raft foundation. The load-displacement curve was compared with a pile raft foundation modeled under axisymmetric conditions. It was observed that the load-displacement curves were reasonably close to each other.

Mandolini *et al.* [8] reviewed pile group behavior under vertical loads in terms of settlement, load distribution, and bearing capacity, through monitoring full scale structures and experimental researches. They concluded that the use of classical methods for foundation design, which was used in practice, was not suitable for a proper design, and needed to be revised. Comodromos *et al.* [5] optimized a foundation design for a bridge, based on both experimental data and non-linear 3D analysis. They analyzed the relationship of load distribution with settlement and throughout the length of the piles, for 2×2 and 3×3 pile group arrangements.

The behavior of the pile group foundation can also be evaluated when it is subjected to excavation-induced soil movement. Analyzing 4-pile groups connected to a pile cap with different rigidity from centrifuge model tests, Choudhury *et al.* [3] concluded that, for a rigid pile cap, the maximum negative bending moment was developed at the head of the pile, and was larger compared to a flexible cap. Furthermore, larger pile head deflection was observed in the pile group with a flexible pile cap, compared to a similar pile group with a rigid pile cap. Very recently, several researchers have performed numerical analyses of modelling of pile group foundations using the adaptive generated mesh approach, including Ninić *et al.* [10], Das and Mehrmann [11], Das [12], Das and Natesan [13], and Mortie [14].

The behavior of pile groups are frequently described by means of load-displacement curves. Only a few have studied the effect of load distribution on the pile group. Those who studied load distribution correlated it with the settlement (Comodromos *et al.* [5]), throughout the pile length (Comodromos *et al.* [5] and Comodromos *et al.* [4]), and the pile diameter (Mandolini *et al.* [8]). In this paper, the relationship between load and pile location is considered. There are very few researches which have studied load distribution of the pile group subjected to a combined vertical load and large moment.

The objective of this paper is to present a 2D finite element analysis of the pile load distribution behavior of a pile group foundation modeled by embedded pile row. The behavior of a single pile case is first analyzed, followed by studying the behavior of the pile group. The load distribution of the pile

group, using finite element analysis and classical static method, is also compared. Parametric studies are also performed to analyze the influence of the number of piles, loading condition, pile spacing, and rigidity of the pile cap, on the behavior of the pile group.

Materials and methods

Site classification

The soil profile considered in this study is located in Nakhon Si Thammarat province, a southern city of Thailand. Based on the soil report for the construction site of the pile group foundation in this province, it is composed of a clay layer, subdivided into 4 general types, as shown in **Figure 3**. The first layer is classified as very soft clay, where its undrained shear strength, s_u, and Young's modulus, E_u, increases linearly from elevation 0m to elevation −15m. The second layer is composed of medium stiff clay, which is from elevation −15 to −20 m. From elevation −20 to −27 m, the soil stratum is made up of stiff clay. The last layer is from elevation −27 to −35 m, classified as hard clay. The second to fourth layers have constant undrained shear strength, s_u, and Young's modulus, E_u, with different magnitudes. The ground water level (G.W.L.) is located 1.50 m below the ground surface. For this study, the pile tip is designed to be located in the hard clay (elevation −27 m). The properties of the soil profile will be presented in subsequent sections of the paper.

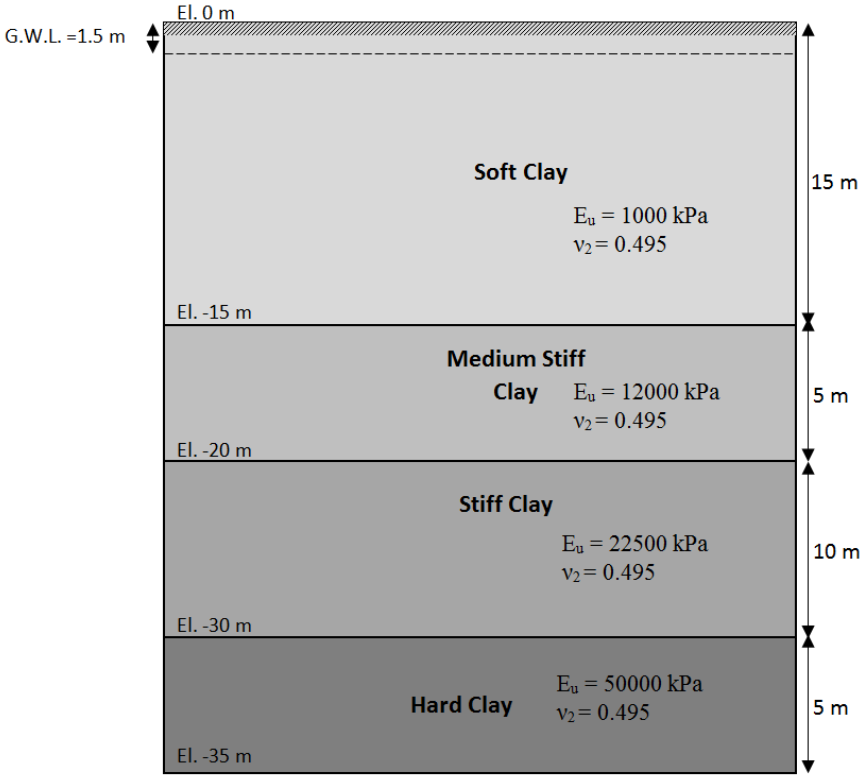

Figure 3 Soil profile of the selected site.

Characteristics of 2D finite element model

In this study, a simplified 2D analysis of the pile group foundation is used by considering the cross section of a strip of pile row, as shown in **Figure 2**. In order to analyze the behavior of the single pile and pile group, subjected to vertical and overturning moment, the finite element software, PLAXIS 2D (Brinkgreve [2]), is used. The finite element analysis is performed under 2 dimensional plane strain conditions. This model is used for geometries with (more or less) the same cross-section and corresponding stress state and loading scheme over a certain length perpendicular to the cross-section (z-direction) 2D (Brinkgreve [2]).

1. Geometry model

Figures 4 and **5** show the geometry model of the single pile and the pile group foundation, respectively. In the case of single pile, the geometry of the numerical model consists of 2 material components: 1) soil elements; and 2) a single embedded pile row. However, for the case of the pile group, the geometry of the numerical model consists of 4 material components: 1) soil elements; 2) a series of embedded pile rows; 3) small vertical pile plate elements; and 4) a plate element for the pile cap. In this case, the plate pile cap and the underlying soil are modeled to have a small gap (0.1 m) between them, in order to simulate the model as the pile group foundation, as shown in **Figure 6**. This modeling is to avoid load transfer from the pile cap to the underlying soil. Without this small gap, the behavior of the problem affects the pile raft foundation, where all applied loads are shared by the underlying soil and piles. With this small gap, the vertical load and overturning moment applied to the pile cap are transferred only to the pile group, without any load sharing of the underlying soils. To model the pile group foundation, a vertical pile plate element connecting the embedded pile row and the plate element of the pile cap is created. It should be noted that the vertical plate segments are set to be weightless, in order to not add any vertical loading to the pile. The connection between the vertical plate and the embedded pile row is a hinged connection, in order to allow only the vertical load transfer from the cap to the embedded pile row, without transferring a bending moment. However, the connection between the vertical plate and the plate pile cap is fully fixed, in order to have an adequate degree of freedom in the entire stable system.

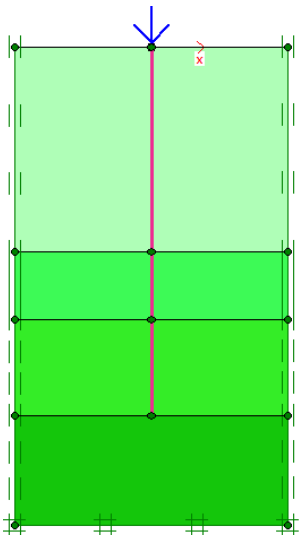

Figure 4 Finite element model of single pile.

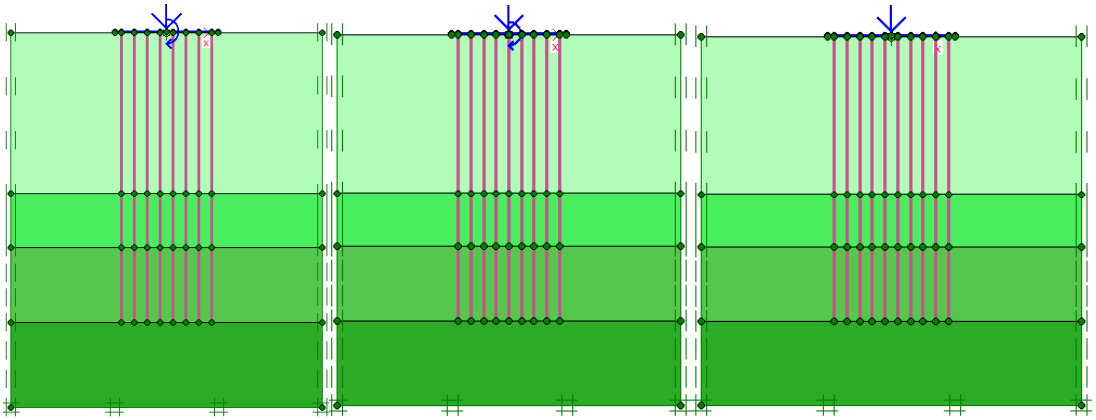

(a) (b) (c)

Figure 5 Finite element model of pile group with 3B pile spacing (a) 8×1, (b) 9×1, and (c) 10×1.

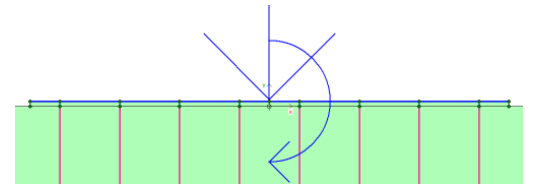

(a)

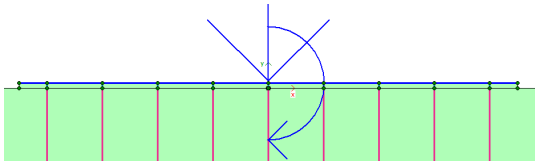

(b)

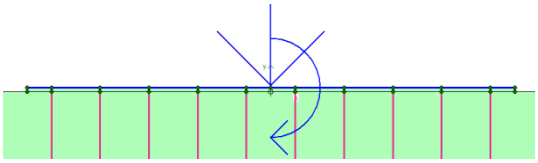

(c)

Figure 6 Modeling techniques for connection between piles and pile caps of (a) 8×1, (b) 9×1, and (c) 10×1 pile group.

2. Element types

The 15-node triangular elements with 12 stress points are used to model the soil layers. The pile cap and vertical piles connecting the pile cap and each individual embedded pile row are modeled using a plate element with 3 degrees of freedom per node: 2 translational degrees of freedom (u_x and u_y), and one rotational degrees of freedom perpendicular to the cross-section (θ_z). Parametric studies are also

performed on pile cap thickness. Two thicknesses were selected, 1.8 and 2.0 m. **Table 2** displays the values for the axial stiffness, *EA*, and flexural rigidity, *EI*, for the respective thicknesses.

The pile rows are modeled using the special element, called the embedded pile row, developed by Sluis [9]. Using this element means that the piles are not 'in' the 2D model, but superimposed 'on' the mesh while the soil element is still continuous. **Figure 7** shows the interaction between the embedded pile row and surrounding soil. The interaction between the embedded pile row and adjacent soil is modeled by the special interface element, which is automatically added around the embedded pile row. Its behavior is of the elastic-plastic Mohr-Coulomb model of the adjacent soil. More details of the embedded pile row can be found in Sluis [9] and Brinkgreve [2].

3. Material properties

The constitutive model used for the soil is the Mohr-Coulomb material in an undrained condition. The elastic isotropic material type is applied for both plate elements of the pile caps and small vertical pile plate elements. A summary of the properties is shown in **Tables 1 - 3**. In this study, the weight of the plate elements of the pile caps is assumed to be zero, but their weight effects are considered by adding their weight to the total vertical applied loads. Generally, the interface roughness (R_{inter}) between piles and soil ranges between 0.5 - 0.95, depending on the undrained shear strength of the clay. Since there is no existing data of the interface roughness in this area, the standard value of interface roughness is chosen to be 0.67, according to the typical value used in the standard practice of pile foundation. It should be noted that the undrained (B) denotes the effective stress analysis of the finite element simulation using the undrained strength parameters, namely $c = s_u$, $\phi = 0$, $\psi = 0$, where c = cohesion, s_u = undrained shear strength, ϕ = total friction angle, and ψ = total dilation angle.

Table 1 Material properties of soil.

Parameter	Symbol (unit)	Soft clay	Medium stiff clay	Stiff clay	Hard clay
Material model	Model	Mohr-Coulomb	Mohr-Coulomb	Mohr-Coulomb	Mohr-Coulomb
Type of material behavior	Type	Undrained (B)	Undrained (B)	Undrained (B)	Undrained (B)
Soil unit weight above phreatic level	γ_{unsat} (kN/m^3)	15.93	15.3	19.3	17.73
Soil unit weight below phreatic level	γ_{sat} (kN/m^3)	15.93	15.3	19.3	17.73
Undrained shear strength	$s_{u,ref}$ (kN/m^2)	10	60	115	125
	$E'/s_{u,ref}$	100	250	400	500
Young's modulus	E' (kN/m^2)	1000	15000	46000	62500
Friction angle	ϕ' (°)	0	0	0	0
Dilatancy angle	ψ (°)	0	0	0	0
Young's modulus inc.	E'_{inc} (kN/m^2)	66.67	-	-	-
Reference level	y_{ref} (m)	0	-	-	-
Undrained shear strength inc.	$s_{u,inc}$ (kN/m^2)	0.67	-	-	-
Reference level	y_{ref} (m)	0	-	-	-
Poisson's ratio	ν'	0.35	0.35	0.35	0.35
Strength reduction factor	R_{inter}	0.67	0.67	0.67	0.67

Table 2 Material properties for plate elements of pile caps and vertical pile plate elements.

Parameter	Symbol	Pile cap	Vertical pile plate	Unit
Material model	Type	Elastic, isotropic	Elastic, isotropic	-
Normal stiffness	EA	4.58×10^7 5.09×10^7	3.39×10^6	kN/m
Flexural rigidity	EI	1.24×10^7 1.07×10^7	4.52×10^7	kNm^2/m
Weight	w	-	-	kN/m/m
Poisson's ratio	ν	0.2	0.2	-

Table 3 Material properties of embedded pile rows.

Parameter	Symbol	Soft clay	Unit
Young's modulus	E	2.54×10^7	kN/m^2
Unit weight	γ	24	kN/m^3
Pile type	-	Pre-defined massive square pile	-
Width	B	0.4	m
Spacing of the piles in the out-of-plane direction	$L_{spacing}$	1.2 1.5	m
Skin resistance at the pile bottom	$T_{bot,\ max}$	0	kN/m
Skin resistance at the pile top	$T_{top,\ max}$	100	kN/m
End-bearing resistance	F_{max}	237.7	kN

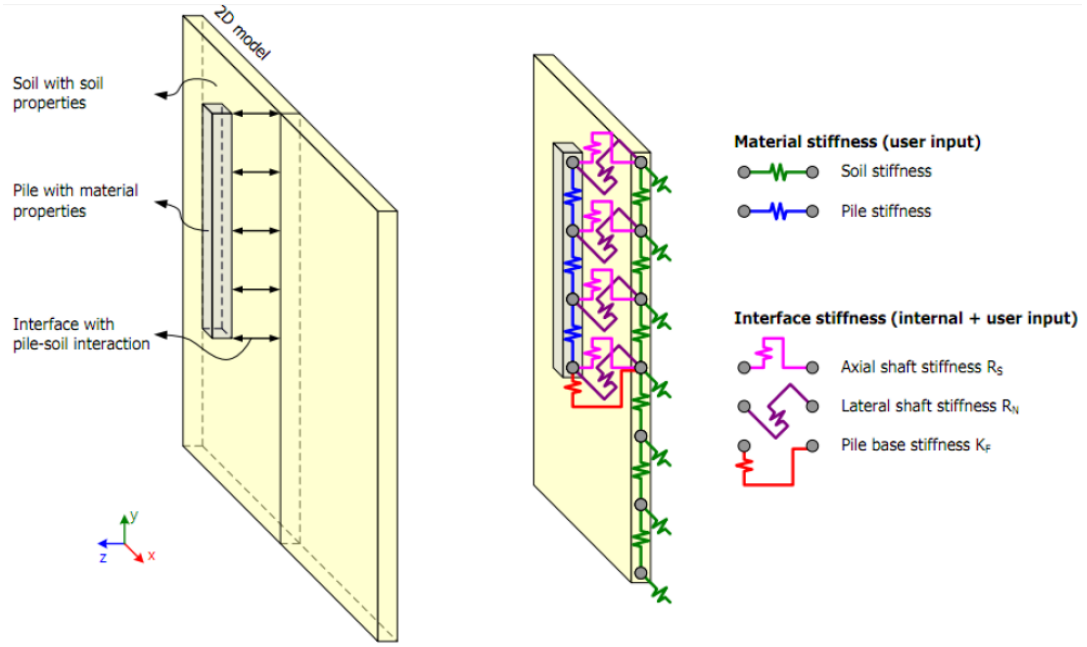

Figure 7 Interaction between soil and embedded pile (Sluis [9]).

4. Parametric studies

Five parametric studies included: 1) a single pile row; 2) multiple pile rows, or a number of piles rows; 3) moment ratios; 4) pile cap stiffness; and 5) pile spacing. The first analysis is of a single pile row without a pile cap, where the load is directly applied to the pile, as shown in **Figure 4**. The second parametric analyses correspond to a pile group consisting of multiple embedded pile rows, having 3 cases: 8×1, 9×1, and 10×1 groups. The third parametric studies consider a purely vertical load and a vertical load with a large overturning moment of 2 ratios applied at the center of the plate element of the pile cap. The fourth parametric study is a variation of pile cap stiffness, where 2 thicknesses are selected, 1.8 and 2.0 m. The last parametric analyses consider 2 ratios of pile spacing: 3.0 and 3.75 times the square pile size, B. **Figure 5** shows the arrangement of 3 pile group cases with 3.0B spacing.

5. Boundary condition and mesh generation

Standard fixity (fixed and roller) boundary conditions are used in the model. To optimize the accuracy and the amount of time required to calculate the load steps, the global coarseness was set to medium mesh refinement. **Figure 8** shows an example of mesh generation for the case of a single pile row and multiple pile rows having coarseness of medium mesh.

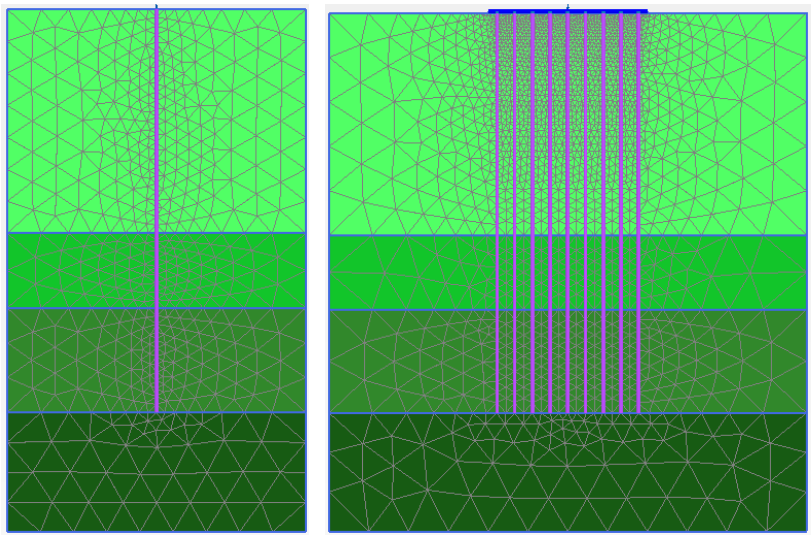

(a) (b)

Figure 8 Mesh generation of pile group having coarseness of medium mesh; (a) single pile row and (b) 9×1.

Static calculation of pile capacity

As shown in **Figure 9**, the ultimate bearing capacity of an individual pile can be calculated as;

$$Q_{ult} = Q_s + Q_E - W_p \quad (2)$$

where, Q_{ult} = ultimate pile capacity
Q_s = ultimate skin resistance of pile = $R_{inter}s_uPL$,
Q_E = ultimate end bearing resistance of pile = $(9s_u+\sigma_{v0})A$
W_p = weight of the pile
P, L = pile perimeter and length, respectively
A = area of pile
σ_{v0} = total overburden pressure at pile tip

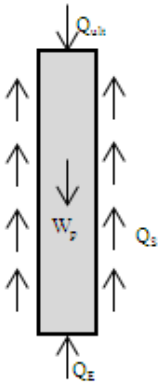

Figure 9 Static calculation of single pile capacity.

The allowable bearing capacity, Q_{all}, is computed by dividing the sum of skin resistance, Q_s, and end bearing resistance, Q_E, by the factor of safety, *FS*, which is 2.5, then subtracting it by the weight of the pile, W_p. **Table 4** summarizes the computed values of pile capacity. In comparing results obtained from this study, the allowable bearing capacity is divided by the out-of-plane spacing of the embedded pile row, S = 1.20 m, which makes the value of the allowable bearing capacity, Q_{all} = 442 kN/m. It should be noted that the pile length of 27 m was chosen based on the result of the allowable pile capacity using the static method with a factor of safety of 2.5.

Table 4 Pile capacity calculation for pile spacing of 1.20 m.

Skin resistance, Q_S (kN)	End-bearing resistance, Q_E (kN)	Weight, W (kN)	Ultimate pile capacity, Q_{ult} (kN)	Q_E/S	Q_{ult}/S	Q_{all}/S
1345	238	104	1479	198.3	1233	442

Moment ratios

There are 3 loading conditions simulated in this study: M/P = 0, M/P = 2.4 and M/P = 2.6. The 2 cases of combined vertical load and moment correspond to some structures of pile group foundation subjected to a very large overturning moment. It should be noted that the maximum computed force of all embedded pile rows, F_{max}, under the serviceability condition, must be less than the allowable pile capacity calculated by the static method. Otherwise, the design input conditions are not valid.

Results and discussion

Single pile case

1. Serviceability state

The behavior of a single pile under the serviceability state is first analyzed. **Figure 10a** shows the deformed mesh of this analysis, where a high degree of shearing happens at the pile-soil interface. It can be observed in **Figure 10b** that, at the serviceability state, the shear stresses are first mobilized at the tip of the pile. A relationship between loads applied in the pile until allowable pile capacity and their corresponding displacement is shown in **Figure 11**. As expected, a linear relationship is observed because of the elastic theory. From the graph, the equivalent pile spring stiffness ($k_{s,eq}$) of the single pile row case can be obtained as: $k_{s,eq} = 63.7 \times 10^3$ kN/m.

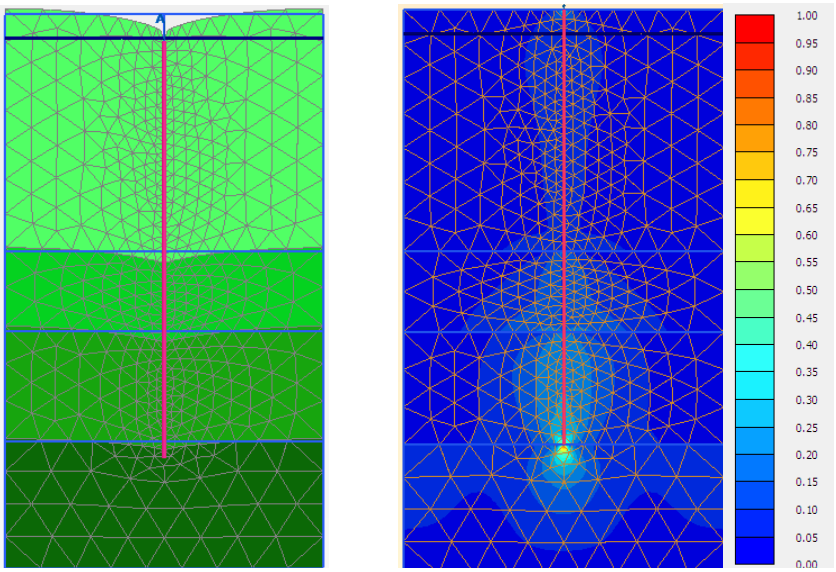

(a) (b)

Figure 10 Results of single pile at serviceability state; (a) deformed mesh and (b) relative shear stress.

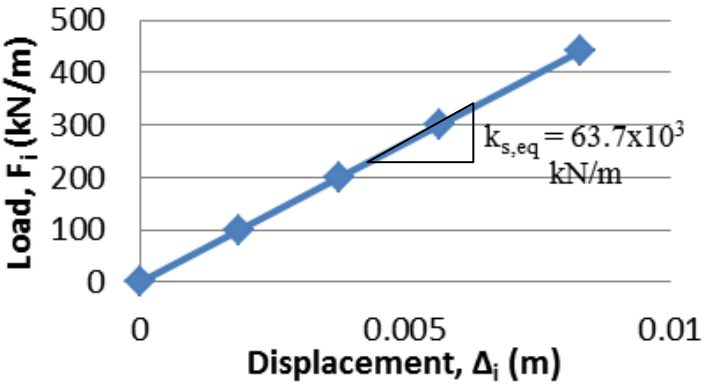

Figure 11 Load-displacement curve of single pile under serviceability state.

2. Limit state of ultimate pile capacity

The behavior of a single pile in the limit state is next examined. **Figure 12a** shows the deformed mesh of this analysis, where complete slippage can be observed at the pile-soil interface. As shown in **Figure 12b**, shear tractions are fully mobilized along the pile length. Similarly, the end bearing stresses underneath the pile are also fully mobilized at its tip. The load-displacement curve is shown in **Figure 13**, indicating that the limit state is successfully solved and reached the convergence. From this figure, the ultimate capacity of a single pile from the analysis is: $P_{ult}/S = M_{stage} \times P_{input} = 0.6209 \times 2000$ kN/m = 1242 kN/m. The reported value of end bearing force, Q_E/S = 198.1 kN/m. It can be seen that the computed values of P_{ult}/S and Q_E/S match very well with those calculated from the static method in **Table 4**. Therefore, these results indicate that the behavior of single pile rows can be analyzed correctly and accurately at the limit state.

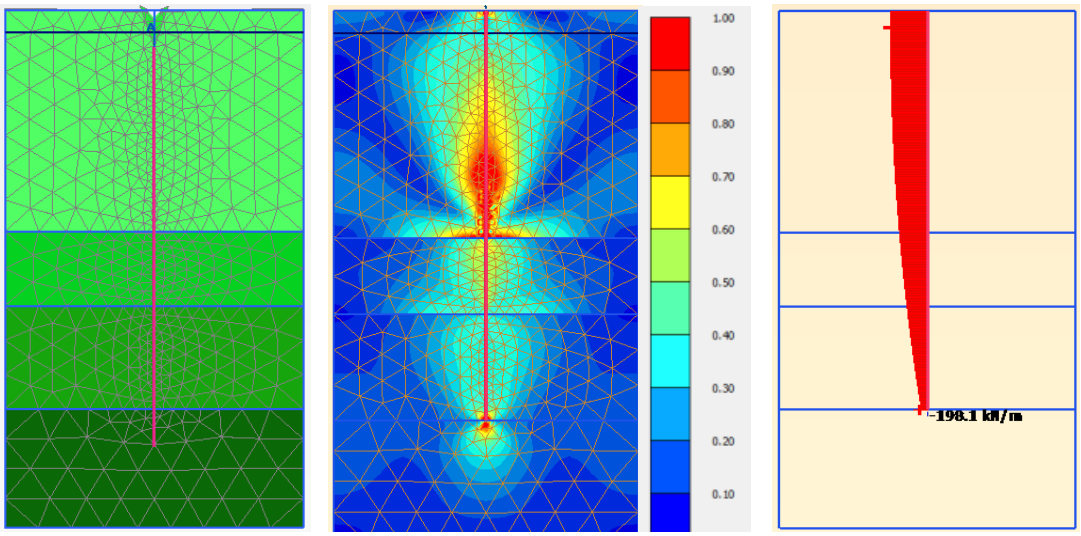

(a) (b) (c)

Figure 12 Results of single pile at limit state; (a) deformed mesh, (b) relative shear stress, and (c) axial force.

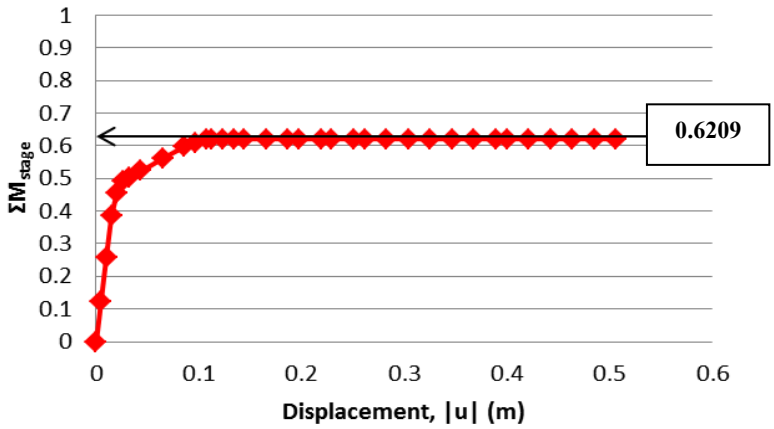

Figure 13 Load-displacement curve of single pile row analysis.

Pile group case

1. Purely vertical load

The base case corresponds to the pile group consisting of pile row 9×1, pile spacing of S = 3B = 1.20 m, and pile cap thickness of 1.8 m. **Figure 14** shows the results of a purely vertical load case. It can be observed that principal effective stress, σ'_1, and relative shear stress, τ_{rel}, are high at the corner piles and at the tip of the pile group. Due to small pile spacing, the soils between piles may have difficulties in moving; hence, the skin capacity of the pile is mainly contributed by the corner piles, which is found to be the same as the result of Engin *et al*. [6]. It should be noted that the load distribution is symmetrical with respect to the center of the pile group.

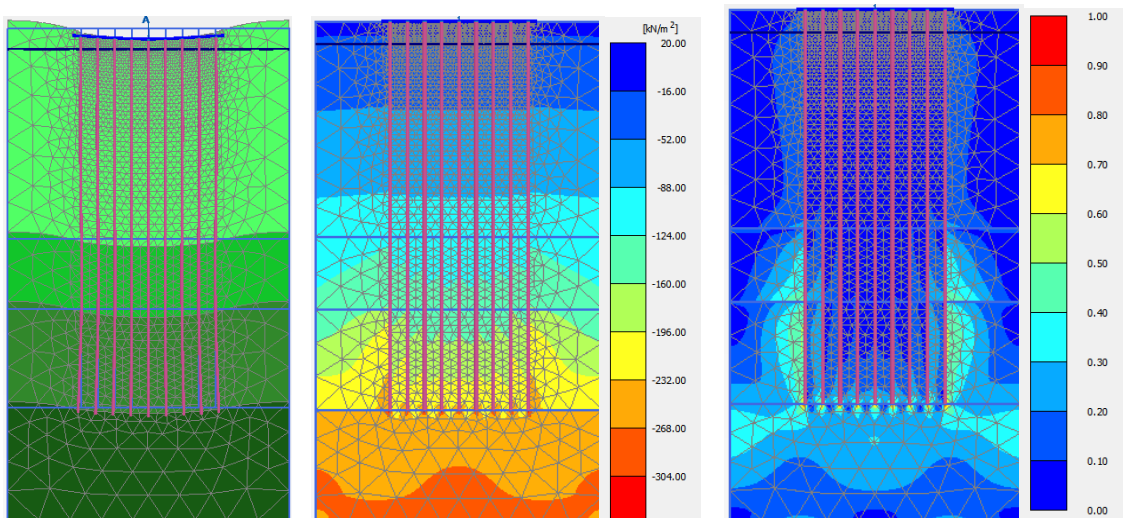

(a) (b) (c)

Figure 14 Results of vertical load of pile group foundation; (a) deformed mesh, (b) principal effective stress, σ'_1, and (c) relative shear stress, τ_{rel}.

The behavior of the load distribution is analyzed by considering 3 normalized plots, as shown in **Figure 15**. For all subplots, the horizontal axis represents the x-position of each pile, x_i, divided by the maximum position, x_{max}, of the exterior pile of the group, giving rise to a range of –1.0 to 1.0. **Figure 15a** shows the distribution of the pile load, F_i, normalized by the maximum computed pile load, F_{max}. **Figure 15b** show the plot of normalized equivalent pile spring stiffness, $k_{i,eq}/k_{s,eq}$, where $k_{i,eq} = F_i/\Delta_i$; Δ_i = settlement of pile i at its top, and $k_{s,eq} = 63.7\times10^3$ kN/m, according to a serviceability state analysis of the single pile row. Lastly, **Figure 15c** shows the normalized settlement profile of the pile cap. It can be seen from those figures that this pile group behaves as if the pile cap is flexible, even though the stiffness of the pile cap is based on 1.8 m. thickness. This result is in contrast to the classical calculation of pile load distribution based on Eq. (1), where all piles carry the same compression load and the pile cap is assumed to be rigid. However, **Figure 15a** shows that the largest pile force is found at the corner piles, while the smallest pile force occurs at the middle pile cap, just below the applied vertical load. **Figure 15b** indicates that the classical assumption of all constant values of equivalent spring stiffness is no longer valid. Each pile behaves as if it has different equivalent spring stiffness, where central piles have softer spring stiffness, but corner piles have stiffer stiffness. Thus, the softer central spring results in larger pile cap settlement, while the stiffer corner spring gives rise to less settlement, as shown in **Figure 15c**. The behavior of the pile group in terms of pile load distribution and equivalent stiffness can be best fitted by a polynomial pattern to the fourth (4^{th}) degree. On the other hand, settlement pattern has a polynomial pattern to the second (2^{nd}) degree.

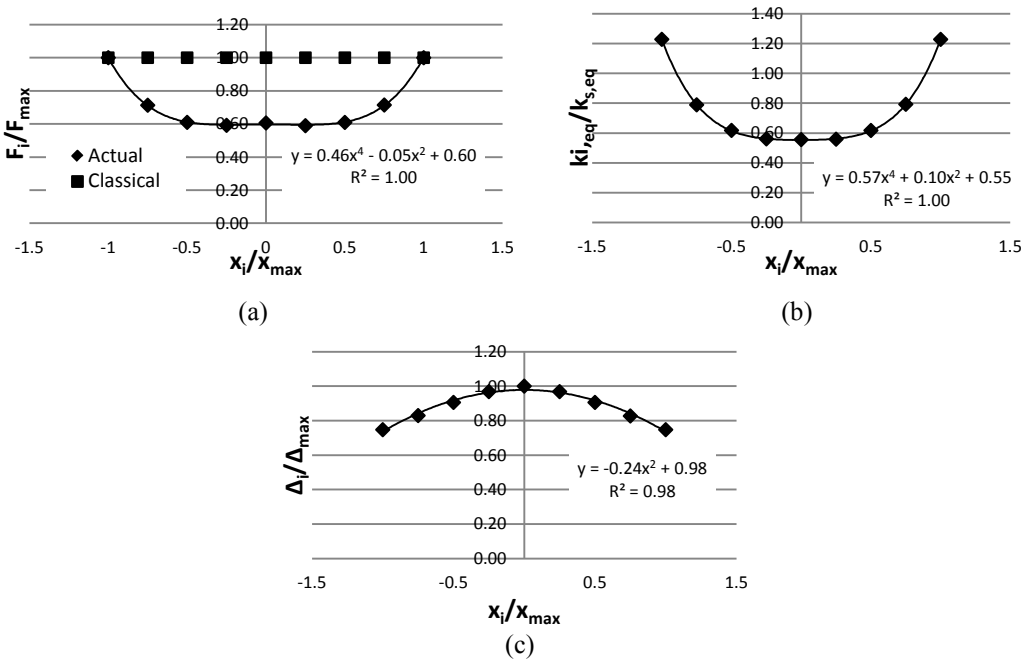

Figure 15 Effect of axial load applied to a pile group of 9 piles; (a) normalized pile load distribution, (b) equivalent pile stiffness, $k_{i,eq}$, and (c) normalized settlement profile.

2. Combined axial load and overturning moment

When the pile group is subjected to a combined axial load and an overturning moment, a change in load distribution is observed. In **Figures 16b** and **16c**, the principal effective stress and relative shear stress are concentrated at the overturning side. It can be observed that piles near the side where moment was applied experience larger principal effective stress and shear stress compared to other piles. In **Figures 17a** and **17b**, larger pile force and settlement are found at the overturning side. Due to a combined axial load and overturning moment, all the piles in the group experience compression. According to the classical calculation in Eq. (1), the load distribution on each pile row is linear, while the behavior for the numerical analysis is polynomial, to the 4th degree. It can be seen that the largest pile load happened at the exterior pile of the same direction of the overturning moment. Comparison of the largest pile load, F_{max} between finite element analysis and the classical calculation is made as follows: Finite element, $F_{max}/P = 0.33$, vs. Classical analysis, $F_{max}/P = 0.24$. It can be clearly seen that using the classical analysis of pile load distribution in Eq. (1) can lead to non-conservative determination of pile force, where some of the pile forces are larger than the allowable capacity. Otherwise, more numbers of piles are required in order to make the design valid. Modeling the accurate behavior of load distribution is important in designing pile groups, since it can lead to overestimation of allowable pile capacity, indicating the design is not valid. As shown in **Figure 17b**, a pile cap settlement profile can be approximated by 2nd order polynomial expression. Again, the classical assumption of a pile cap moving rigidly is no longer valid.

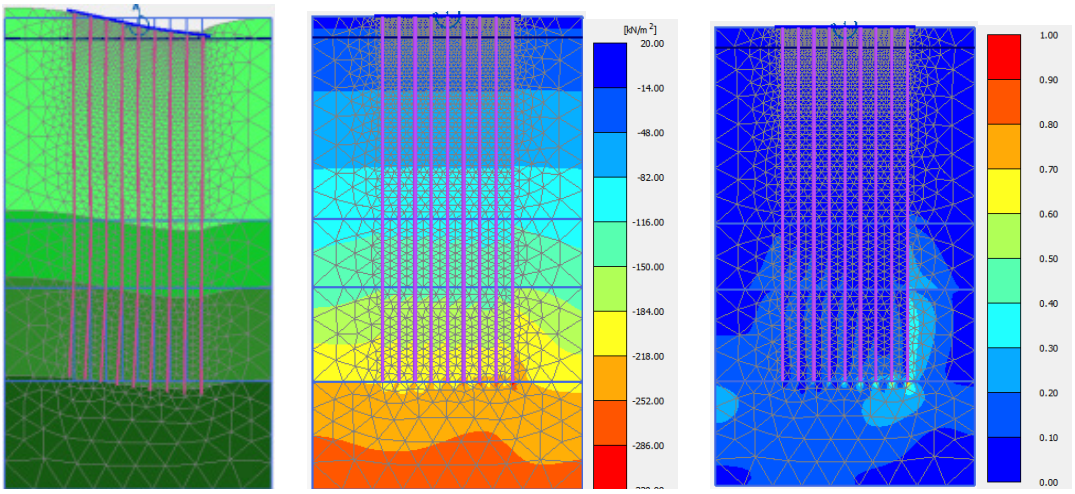

(a) (b) (c)

Figure 16 Results of combined axial load and moment of pile group foundation; (a) deformed mesh, (b) principal effective stress, σ'_1, and (c) relative shear stress, τ_{rel}.

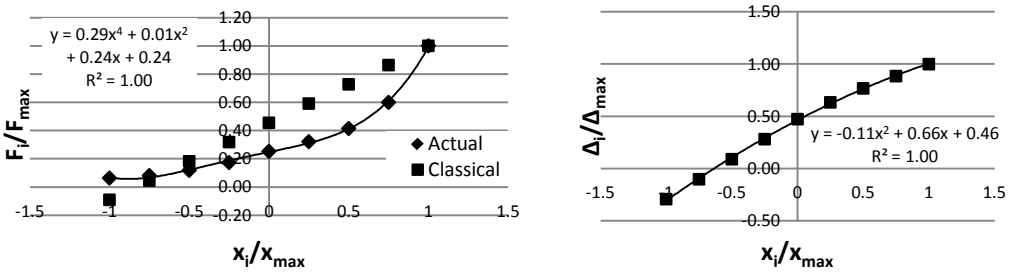

(a) (b)

Figure 17 Effect of combined axial load and moment applied to the pile group; (a) normalized pile load distribution and (b) normalized settlement profile.

Parametric studies on pile group

1. Moment ratios applied to the pile group (M/P)

Parametric analyses are also conducted to examine the consequences of the influence of different factor, namely moment ratios, number of piles, pile cap thickness, and pile spacing on the pile load distribution and settlement profile of the cap. For a typical case with 9 numbers of piles, pile spacing, S = 3B = 1.20 m, and pile cap thickness of 1.8 m, 2 moment ratios, M/P = 2.4 and 2.6, are investigated. It can be seen from **Figure 18** that the pile force distribution and settlement profile can be uniquely normalized with the same trend and with very small differences in the 2 curves.

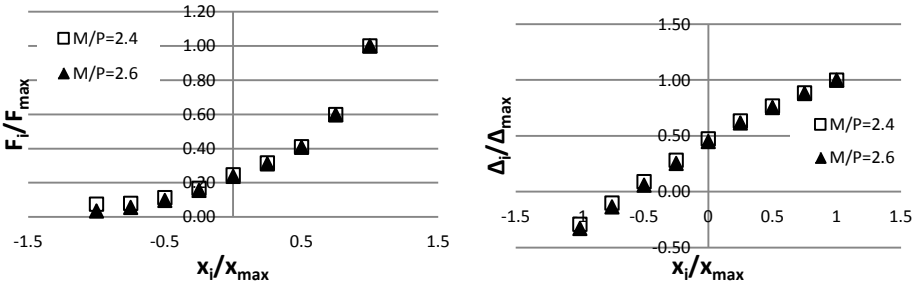

(a) (b)

Figure 18 Influence of moment ratio; (a) normalized pile load distribution and (b) normalized settlement profile.

2. Number of piles

Three configurations are also analyzed in this study: 8×1, 9×1, and 10×1 pile groups. **Figure 19** and **20** show results of analyses regarding normalized pile load distribution and a normalized settlement profile of the cap. Generally, curves of normalized pile load distribution and settlement profiles are not perfectly unique, with small differences observed. The case of a purely vertical load shows larger differences of curves than those of a vertical load with a large moment.

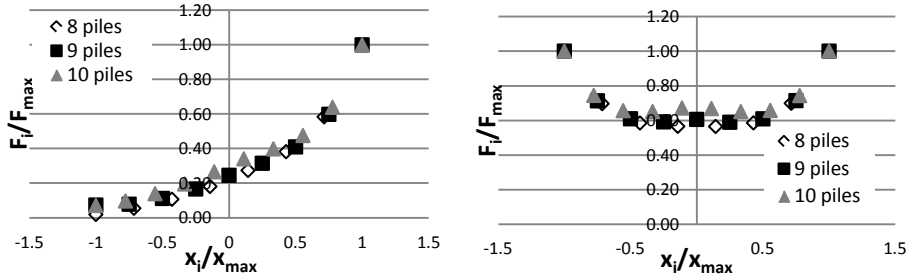

(a) (b)

Figure 19 Influence of number of piles on the normalized pile load distribution; (a) combined axial load and moment case and (b) axial load case.

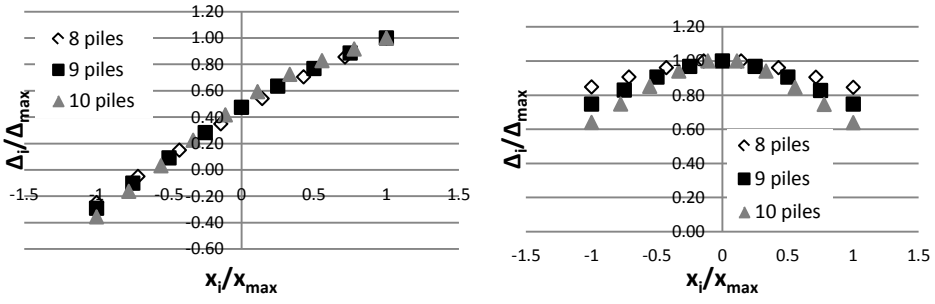

(a) (b)

Figure 20 Influence of number of piles to the normalized settlement profile; (a) combined axial load and moment case and (b) axial load case.

3. Pile cap thickness

There are 2 pile cap thicknesses considered in this study: 1.8 and 2 m. When the thickness varies, the flexural rigidity of the plate element of the pile cap, EI, changes accordingly. A larger pile cap thickness creates a more rigid pile cap. **Figure 21** summarizes the results of pile cap thickness effect. Generally, the curves of the pile load distribution and pile cap settlement were uniquely normalized for 2 different thickness cases.

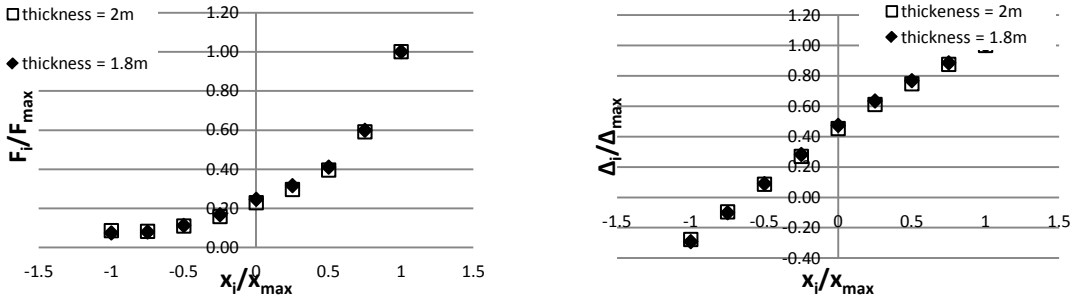

(a) (b)

Figure 21 Influence of pile cap thickness; (a) normalized pile load distribution and (b) normalized settlement profile.

4. Spacing of piles

The last parametric analyses focus on the influence of the pile spacing on the behavior of the pile group. In **Figure 22**, it can be observed that larger pile forces are developed at intermediate piles by increasing the spacing between piles. The effect of pile spacing is more significant than other parameters, as described earlier. In general, the curves of the pile load distribution and the settlement profile of the cap cannot be uniquely normalized. However, when the pile group is subjected to a combined vertical load and moment, the pile spacing does not affect the behavior of the settlement.

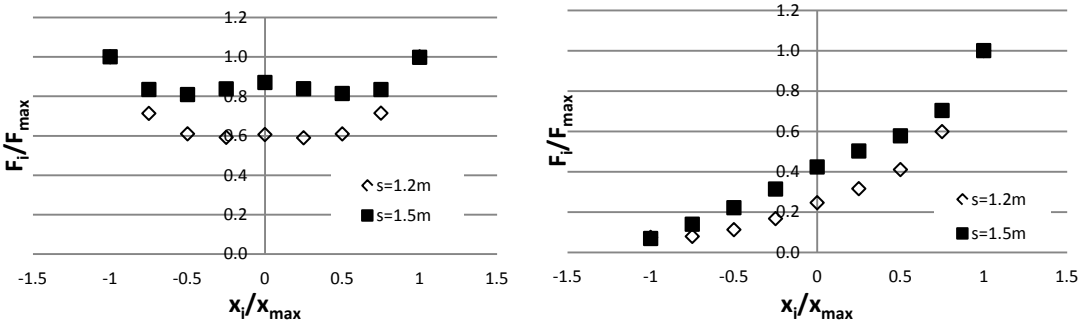

(a) (b)

Figure 22 Influence of spacing of piles on the normalized pile load distribution; (a) axial load case and (b) combined axial load and moment case.

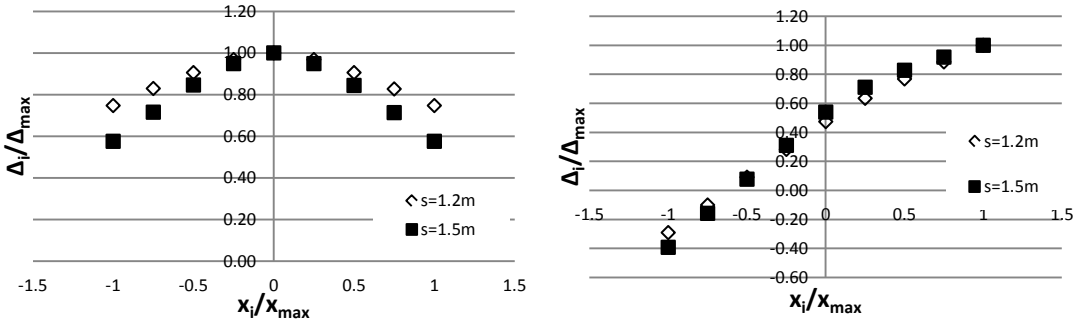

(a) (b)

Figure 23 Influence of spacing of piles on the normalized settlement profile; (a) axial load case and (b) combined axial load and moment case.

Conclusions

This paper presents numerical investigations of 2D modeling of a single pile row and multiple pile rows of pile group foundations by 2 dimensional plane strain finite element analysis, together with an embedded pile row element. It is concluded that the use of a single pile row model to describe the behavior at the limit state is accurate and comparable to the static method. For cases of vertical load and combined vertical load and a large overturning moment, the load distribution behaviors of the pile group are found to be different, compared to those of rigid pile cap assumption. The present classical method predicting the behavior of the pile group foundation may not be sufficient, as this method can predict pile loads smaller than those of more realistic analyses, such as finite element methods. For a purely vertical load case, the behavior of the normalized pile load distribution and equivalent pile spring stiffness can be best fitted by a 4^{th} degree polynomial expression, while the normalized settlement profile of the pile cap is well approximated by a 2^{nd} degree polynomial pattern. Moreover, individual piles developed different equivalent spring stiffness, whereas intermediate piles behaved as soft springs and corner piles behaved as stiff springs. For a combined vertical load and moment case, the curves of pile load distribution and settlement of pile cap are quite unique, with some minor differences in different parameters of number of piles, stiffness of pile cap, and moment ratios. However, pile spacing is the most significant parameter, where pile load distribution does not turn out to be a unique curve.

References

[1] JE Bowles. *Foundation Analysis and Design*. McGraw-Hill, Singapore, 1988.
[2] RBJ Brinkgreve. *Plaxis 2D 2012 Manual*. A.A. Balkema Publishers, Netherlands, 2012.
[3] D Choudhury, RF Shen and CF Leung. *Centrifuge Model Study of Pile Group Subject to Adjacent Excavation*. GeoCongress, Louisiana, United States, 2008, p. 141-8.
[4] EM Comodromos, CT Anagnostopoulos and MK Georgiadis. Assessment of axial pile group response based on load test. *Comput. Geotech.* 2003; **30**, 505-15.
[5] EM Comodromos, MC Papadopoulou and IK Rentzeperis. Pile foundation analysis and design using experimental data and 3-D numerical analysis. *Comput. Geotech.* 2009; **36**, 819-36.
[6] HK Engin, EG Septanika and RBJ Brinkgreve. Estimation of pile group behavior using embedded piles. *In*: Proceeding of the 12^{th} International Conference of International Association for Computer Methods and Advances in Geomechanics, Goa, India, 2008, p. 3231-8.
[7] FE-Analysis of Piled and Piled Raft Foundations, Available: http://kb.plaxis.nl/sites/kb.plaxis.nl/files/kbpublications/tschuchnigg_lebeau_validation_emb_pile.pdf, accessed July 2015.

[8] A Mandolini, G Russo and C Viggiani. Pile foundations: Experimental investigations, analysis and design. *In*: Proceeding of the 16th International Conference on Soil Mechanics and Geotechnical Engineering, Osaka, Japan, 2005, p. 177-213.
[9] J Sluis. Validation of Embedded Pile Row in Plaxis 2D, Available: http://kb.plaxis.com/publications/validation-and-application-embedded-pile-row-feature-plaxis-2d, accessed October 2015.
[10] J Ninić, J Stascheit and G Meschke. Beam-solid contact formulation for finite element analysis of pile-soil interaction with arbitrary discretization. *Int. J. Numer. Anal. Meth. Geomech.* 2014; **38**, 1453-76.
[11] P Das and V Mehrmann. Numerical solution of singularly perturbed convection-diffusion-reaction problems with two small parameters. *BIT Numer. Math.* 2016; **56**, 51-76.
[12] P Das. Comparison of a priori and a posteriori meshes for singularly perturbed nonlinear parameterized problems. *J. Comput. Appl. Math.* 2015; **290**, 16-25.
[13] P Das and S Natesan. Richardson extrapolation method for singularly perturbed convection-diffusion problems on adaptively generated mesh. *Comput. Model. Eng. Sci.* 2013; **90**, 463-85.
[14] I Mortie. 2014, Numerical Analysis of Slope Stability Reinforced by Piles in Over-Consolidated Clay. Master Dissertation. Ghent University, Belgium.